

# Direct-search deep level photothermal spectroscopy: An enhanced reliability method for overlapped semiconductor defect state characterization

Jun Xia and Andreas Mandelis<sup>a)</sup>

Department of Mechanical and Industrial Engineering, Center for Advanced Diffusion-Wave Technologies (CADIFT), University of Toronto, Toronto, Ontario M5S 3G8, Canada

(Received 11 March 2010; accepted 5 June 2010; published online 1 July 2010)

A method for resolving highly overlapped defects in rate-window analysis is proposed. This method offers high defect-state characterization reliability because it is based on direct multiparameter fitting of deep level photothermal spectra using combined temperature and frequency scans. Two direct search optimization algorithms are utilized as follows: the genetic algorithm for a search of possible solution areas and the pattern search algorithm for a refined search of global minimum. Four defect levels are identified using this technique. © 2010 American Institute of Physics. [doi:10.1063/1.3458827]

Deep-level transient spectroscopy (DLTS), first introduced by Lang,<sup>1</sup> is a very useful technique for characterizing deep level defects in semiconductor materials. The principle of DLTS is based on an ideal configuration that defect states have discrete activation energies and each defect gives a peak in DLTS spectra. However, in real semiconductor systems, it is commonly observed that defect activation energies can be broadened due to potential fluctuations<sup>2</sup> or constrained emission processes,<sup>3</sup> and several defect peaks may merge into a single broadened peak. In this case, the conventional Arrhenius plot cannot be applied.

The analysis of multiexponential decays in defect relaxation has been a long-standing issue due to the ill-posed nature of the problem.<sup>4</sup> Currently, the best energetic resolution is obtained from LAPLACE DLTS,<sup>5,6</sup> which is based on the inverse Laplace transform of exponential decays. This method, however, requires a careful and time-consuming extraction of the transient baseline, usually by sampling the transient long enough until all defect states are completely depleted. Instrumental fluctuations may also enter the signal during transient sampling and further add inaccuracies in determining defect parameters.<sup>4</sup> For these reasons, the conventional lock-in-amplifier (LIA) is still widely used as an effective tool for rate-window analysis. In this paper, a fitting technique is proposed in combined temperature and frequency-scanned LIA deep-level photothermal spectroscopy (DLPTS) (Ref. 7) for resolving highly overlapped defects.

As mentioned earlier, conventional DLTS is based on Arrhenius plots of contributing defect peaks. When there is only one peak, multiple defects can only be resolved from the direct multiparameter fits of experimental spectra. The principle of this fitting is to find the minimum difference between theoretical and experimental data by adjusting a number of parameters, which in our case are the defect parameters.

The theoretical model used in our study is the simplified carrier-rate theory, which has been widely used in GaAs defect analysis.<sup>8</sup> Broadening effects are simulated by the hierarchical carrier emission model expressed in the form of a stretched exponential decay<sup>3</sup>

$$n_T(t) \propto \exp\{-[e_{n0}(T)t]^\beta\}; \quad \beta(T) = \left(1 + \frac{\Delta E_0}{k_B T}\right)^{-1}. \quad (1)$$

Here  $\Delta E$  indicates the magnitude of defect broadening. Compared with the Gaussian broadening model,<sup>2</sup> the hierarchical emission model has inherent advantages for multiparameter fitting since it does not include integrals and can significantly reduce the computational time.

Since each defect level contributes equally to the system, it is necessary to add inequality constraints as shown in Eq. (2). This will avoid the calculation of defect states with the same activation energy but different capture cross sections. Here, 0.03 eV is the limit of resolving two closely located broadened defects  $m$  and  $(m-1)$

$$E_m - E_{m-1} \geq 0.03 \text{ eV}. \quad (2)$$

Selection of the optimization algorithm is also very important for the fitting. Due to the complexity of our model and the large number of fitting parameters, the direct search

TABLE I. Defect parameters for the simulated DLPTS spectra in Fig. 1.

Defect No.	1	2	Search range
$E_n$ (eV)	0.6	0.55	0.30–0.8
$N_T$ ( $\times 10^{16}$ cm <sup>3</sup> )	1	0.8	0.01–10
$\sigma_n$ ( $\times 10^{-13}$ cm <sup>2</sup> )	1	2	0.01–50
$\Delta E$ (meV)	10	20	0.1–100

TABLE II. Accuracy of defect parameter identification.

	$E_n$ (%)	$\sigma_n$ (%)	$\Delta E$ (%)	$N_T$ (%)
Temperature scan (amplitude and phase)	99.9	97.9	98.8	98.2
Frequency scan (amplitude and phase)	99.5	97.4	92.5	96.4
Temperature and frequency scans	99.8	99.4	95.0	99.8

<sup>a)</sup>Electronic mail: mandelis@mie.utoronto.ca.

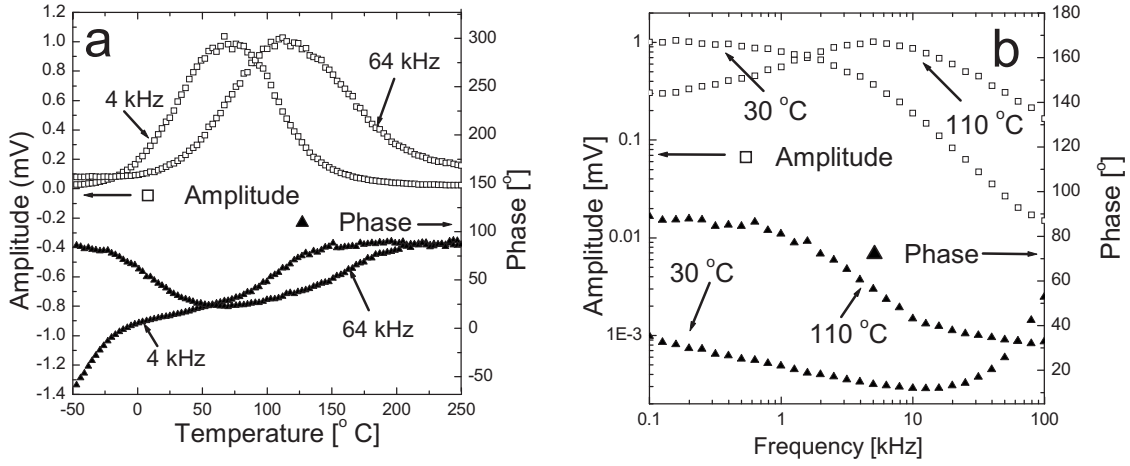


FIG. 1. The theoretical DLPTS (a) temperature-scanned spectra and (b) frequency-scanned spectra.

method, which does not rely on derivative operations, is used for our study.<sup>9</sup> In order to avoid the arbitrary guess of initial values, the genetic algorithm (GA),<sup>10</sup> which can generate randomized initial values, is used for locating the possible solution area. Due to the nature of randomized genetic operations, the GA exhibits very slow convergence and is not efficient in finding the global minimum.<sup>11</sup> For this reason, the GA program is hybridized with a more efficient local optimization algorithm. In this study, due to the inequality [Eq. (2)] constraints, we choose the pattern search algorithm whose convergence in constraint problems has been well studied.<sup>12</sup> Both genetic and pattern search algorithms can search within a defined boundary as shown in Table I.

Since defect peaks are highly overlapped, it is difficult to resolve them from a single temperature scan. For this reason, multiple temperature- and frequency-scanned measurements are performed. The fitting is therefore performed on a three-dimensional space comprising two independent parameters (temperature and modulation frequency) and a third dependent parameter (DLPTS amplitude or phase), which can provide higher reliability in defect identifications than existing methodologies. Both amplitude and phase spectra are fitted in order to get a better recovery of the raw DLPTS signal. The function to be minimized is then defined as

$$Var = \frac{\sum_{i=1}^N (A_T - A_E)^2}{\sum_{i=1}^N (A_E)^2} + \frac{\sum_{i=1}^N (\phi_T - \phi_E)^2}{\sum_{i=1}^N (\phi_E)^2}, \quad (3)$$

where  $A_T \equiv \sqrt{X^2 + Y^2}$  and  $\phi_T \equiv \tan^{-1}(Y/X)$  are the theoretical DLPTS amplitude and phase, and  $A_E$  and  $\phi_E$  are the experimental DLPTS amplitude and phase, respectively.  $N$  is the total number of data points,  $X$  and  $Y$  are the in-phase and quadrature components of the DLPTS signal, respectively.<sup>13</sup>

To test the technique, our fitting is first performed on simulated spectra of two defects shown in Fig. 1. The signal consists of two temperature scans and two frequency scans as indicated in the figure. The defect parameters used for generating the spectra are listed in Table I. Noise is randomly generated and added to the data for a better simulation of experimental conditions. It can be seen that due to broadening both temperature and frequency-scanned spectra show only one peak.

Since the number of defects is unknown in real conditions, our fitting starts with one defect level and then we gradually increase the number of defects until a good fit is obtained. Our fitting indicates that the change in variance is very small when the defect number is higher than two. Therefore we can conclude that the system has two defect states, which is consistent with the theoretical value in Table I.

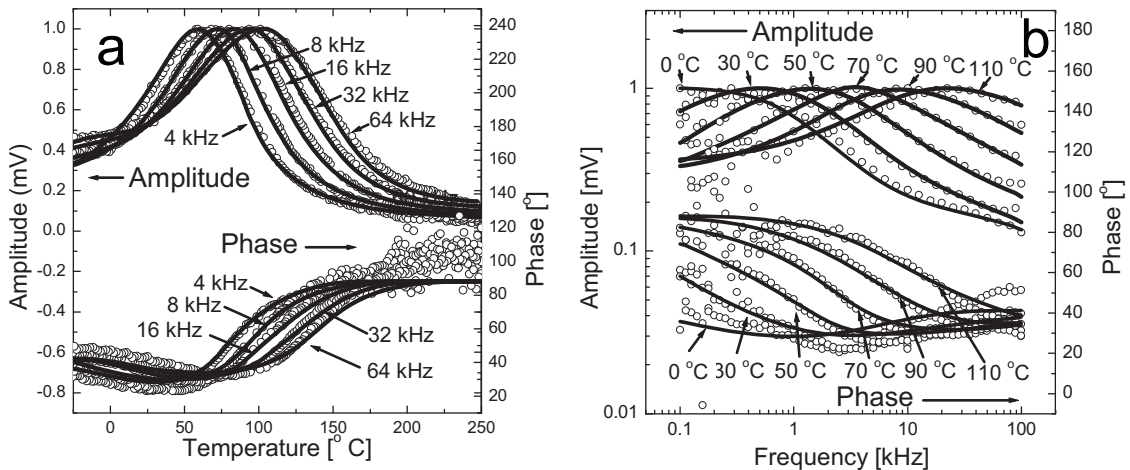


FIG. 2. Experimental and theoretical (a) temperature-scanned DLPTS SI-GaAs spectra and (b) frequency-scanned DLPTS SI-GaAs spectra.

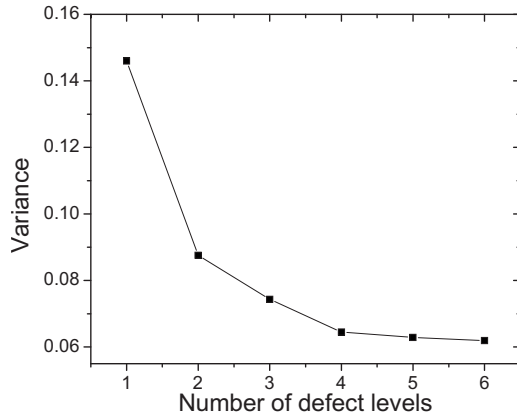


FIG. 3. Change in variance for different number of defects.

The above fitting is performed on both temperature- and frequency-scanned spectra. To evaluate the influence of different experimental modalities, the fitting accuracy, defined in Eq. (4), is utilized as follows:

$$\text{Accuracy} = 1 - |P_{\text{real}} - P_{\text{fit}}|/P_{\text{real}}. \quad (4)$$

Table II shows the fitting accuracy of different DLPTS channels. It can be seen that all approaches give precise determination of defect parameters. The high accuracy is mainly due to the high signal-to-noise ratio of the theoretically generated data. When the noise increases, it is found that both temperature and frequency-scanned data may give rise to nonunique fitting results. Then improved defect-state characterization reliability can only be obtained after combining the outcomes of the two independent experimental modalities. This also demonstrates the power of our DLPTS technique which can be adapted to various experimental conditions to satisfy needs specific to (industrial) substrate and device quality.

LAPLACE DLPTS was also considered. The FTIKREG program<sup>14</sup> was used to fit the transient generated using defect parameters shown in Table I. The fitted spectrum shows four peaks (instead of two), and none of the peaks corresponds to the true emission rate. This is consistent with our previous observations that time domain analysis is less sensitive than temperature and frequency domain studies.<sup>3</sup>

Our experimental data were fitted next. The sample used for the measurement is a vertical gradient freeze-grown GaAs provided by AXT Inc. A detailed discussion of the experimental setup can be found in our earlier papers.<sup>3,7</sup> Both temperature- and frequency-scanned DLPTS spectra shown in Fig. 2 are utilized for the fitting. Here, the amplitudes of temperature and frequency scanned spectra are normalized according to the maximum peak value at each frequency and temperature, respectively.

Similar to the aforementioned theoretical studies, the fitting starts from one defect and the defect number gradually increases until the variance does not change significantly. Figure 3 shows the minimum *Var* versus defect number. It can be seen that the variance decreases gradually as the defect number increases and the change in *Var* is very small for  $n > 4$  defects. This indicates that the noise level of the experimental data has been reached. Therefore we can conclude that there are four measurable defect levels in the system. The fitting parameters are summarized in Table III. Using these parameters, the theoretical spectra were gener-

TABLE III. Summary of identified defect parameters.

Defect No. (identification)	1(HB5)	2(EL5)	3(EL3)	4(HL3)
$E_n$ (eV)	0.39	0.48	0.59	0.63
$N_T$ ( $\times 10^{16}$ cm <sup>3</sup> )	0.13	0.45	0.11	0.21
$\sigma_n$ ( $\times 10^{-13}$ cm <sup>2</sup> )	49.1	0.36	3.0	49.9
$\Delta E$ (meV)	100	36	6.4	73.3

ated and are also presented in Fig. 2 as solid lines. Special attention must be paid to the uniqueness of the fitting results. During fitting, we observed that the optimization algorithm may be trapped at a local minimum depending on the initial value provided by the GA and the chance for that increases as the defect number increases as follows: for instance, the chance is 40% for four defect states while it is 60% for five defect states. Therefore, it is important to apply the GA several times over to ensure that fitting yields the global minimum. It should be noticed that the reliability of the fitting has been improved substantially by combining the temperature- and frequency-scans, thus minimizing the chance of being trapped in a local minimum when fitting either one of the channels. Further improvements can be obtained by using a grid search of the initial values,<sup>15</sup> however, that will significantly increase the computational time and is therefore not performed in this study.

We have developed a DLPTS signal processing technique based on the direct-search optimization algorithm. The technique does not require initial information on the defect states and is capable of resolving defects from a broadened DLPTS spectrum. The technique was first tested using simulated spectra and was then applied to the experimental data leading to the identification of four defect levels. The salient feature of this technique is the substantial improvement in the reliability of defect state characterization by combining the outcomes of two independent DLPTS experimental modalities (temperature- and frequency-scan). We also found that the conventional transient analysis has the lowest sensitivity in defect characterization as the most robust defect extraction methodology associated with transient analysis, the inverse Laplace transform, gave erroneous defect state results for the simulated data and for SI-GaAs.

The authors are grateful to the Natural Sciences and Engineering Research Council of Canada (NSERC) for a Discovery Grant and to the Canada Research Chairs for support of this project.

<sup>1</sup>D. V. Lang, *J. Appl. Phys.* **45**, 3023 (1974).

<sup>2</sup>A. Das, V. A. Singh, and D. V. Lang, *Semicond. Sci. Technol.* **3**, 1177 (1988).

<sup>3</sup>J. Xia and A. Mandelis, *J. Appl. Phys.* **105**, 103712 (2009).

<sup>4</sup>A. A. Istratov and O. F. Vyvenko, *Rev. Sci. Instrum.* **70**, 1233 (1999).

<sup>5</sup>L. Dobaczewski, P. Kaczor, I. D. Hawkins, and A. R. Peaker, *J. Appl. Phys.* **76**, 194 (1994).

<sup>6</sup>L. Dobaczewski, A. R. Peaker, and K. B. Nielsen, *J. Appl. Phys.* **96**, 4689 (2004).

<sup>7</sup>J. Xia and A. Mandelis, *Appl. Phys. Lett.* **90**, 062119 (2007).

<sup>8</sup>D. C. Look, in *Semiconductors and Semimetals*, edited by R. K. Willardson and A. C. Beer (Academic, New York, 1983), Vol. 19, p. 75.

<sup>9</sup>T. G. Kolda, R. M. Lewis, and V. Torczon, *SIAM Rev.* **45**, 385 (2003).

<sup>10</sup>J. H. Holland, *J. ACM* **9**, 297 (1962).

<sup>11</sup>R. Chelouah and P. Siarry, *Eur. J. Oper. Res.* **148**, 335 (2003).

<sup>12</sup>R. M. Lewis and V. Torczon, *SIAM J. Optim.* **12**, 1075 (2002).

<sup>13</sup>A. Mandelis and J. Xia, *J. Appl. Phys.* **103**, 043704 (2008).

<sup>14</sup>J. Weese, *Comput. Phys. Commun.* **69**, 99 (1992).

<sup>15</sup>A. Matvienko, A. Mandelis, and S. Abrams, *Appl. Opt.* **48**, 3192 (2009).